Journal of Orthopaedic Translation (2019) 18, 142–153

Available online at www.sciencedirect.com

ScienceDirect

journal homepage: http://ees.elsevier.com/jot

ORIGINAL ARTICLE

Muscle injury promotes heterotopic ossification by stimulating local bone morphogenetic protein-7 production

La Li [a,b], Yangzi Jiang [a,☆], Hang Lin [a], He Shen [a], Jihee Sohn [a], Peter G. Alexander [a], Rocky S. Tuan [a,b,*]

[a] *Center for Cellular and Molecular Engineering, Department of Orthopaedic Surgery, University of Pittsburgh School of Medicine, Pittsburgh, PA, USA*
[b] *Graduate Program of Cellular and Molecular Pathology, Department of Pathology, University of Pittsburgh School of Medicine, Pittsburgh, PA, USA*

Received 5 March 2019; received in revised form 3 June 2019; accepted 5 June 2019
Available online 5 July 2019

KEYWORDS
Bone morphogenetic protein;
Heterotopic ossification;
Inflammation;
Macrophages;
Muscle injury;
Stromal/stem cells

Abstract *Background:* Heterotopic ossification (HO) is a pathological condition of abnormal bone formation in soft tissue, which causes pain and restricted range of motion in patients. There are two broad categories of HO, hereditary and acquired. Although different types of HO do not use identical mechanistic pathways of pathogenesis, muscle injury appears to be a unifying feature for all types of HO. However, little is known about the mechanisms by which muscle injury facilitates HO formation.
Objective and method: This study aimed to explore the cellular and molecular mechanisms linking muscle injury to HO by using cardiotoxin to induce muscle injury in a bone morphogenetic protein-2 (BMP-2)–induced HO mouse model.
Results: We found that muscle injury augmented HO formation and that this effect was correlated with BMP signalling activation and upregulation of BMP-7 expression at the early phase of HO progression. We further demonstrated that inhibition of BMP-7 activity *in vitro* suppressed the osteogenesis-promoting effect of conditioned medium derived from injured muscle tissue and *in vivo* reduced the volume of HO formation. We also showed that antiinflammatory drug treatment reduced the volume of HO with concomitant reduction in BMP-7 production.
Conclusion: In summary, our study has identified BMP-7 as a key osteoinductive factor in injured muscle that facilitates HO formation.

* Corresponding author. Center for Cellular and Molecular Engineering, Department of Orthopaedic Surgery, University of Pittsburgh School of Medicine, Pittsburgh, PA, USA.
E-mail address: rst13@pitt.edu (R.S. Tuan).
☆ Present address: Institute for Tissue Engineering and Regenerative Medicine, School of Biomedical Sciences, Faculty of Medicine, The Chinese University of Hong Kong, Hong Kong S.A.R., China.

https://doi.org/10.1016/j.jot.2019.06.001

The translational potential of this article: Our results provide a candidate mechanistic rationale for the use of antiinflammatory drugs in the prevention of HO.

Introduction

Heterotopic ossification (HO) is a pathological condition of abnormal bone formation in soft tissue, which causes pain and restricted range of motion in patients [1]. HO can be generally divided into two broad categories: hereditary and acquired. Hereditary HO, also known as fibrodysplasia ossificans progressiva, results from activin A receptor type I (*ACVR1*) gene mutation, a bone morphogenetic protein (BMP) type I receptor that renders constitutive activation of BMP signalling [2]. Acquired HO typically follows central nervous system injury (neurogenic HO) or direct muscular trauma (traumatic HO) [3]. Although these different types of HO do not use identical mechanistic pathways of pathogenesis, muscle injury appears to be a unifying feature for all types of HO. In patients with fibrodysplasia ossificans progressiva, low levels of muscular trauma after childhood immunizations or play-related falls can result in HO [4]. In neurogenic HO, microtrauma to muscles resulting from forced passive movements after a period of immobilization will lead to an increased risk of HO [5]. In traumatic HO, more severe levels of muscular trauma, as in cases of arthroplasty and blast trauma, can lead to an HO incidence of 20% and 64.6%, respectively [6,7]. Muscle injury usually incurs an inflammatory response, and antiinflammatory drugs have been used as prophylaxis in HO-susceptible patients [8,9]. However, the precise mechanism by which muscle injury facilitates HO formation and the mechanistic rationale for the use of antiinflammatory drugs in the prevention of HO are still largely unknown.

In experimental animal HO models, cardiotoxin (CTX) injection has been commonly used to induce muscle injury and subsequent HO. CTX belongs to the family of snake venom polypeptide toxins that cause depolarization and contraction of muscle fibres [10]. Eventually, CTX causes muscle degeneration through myocyte death, which subsequently elicits a regenerative response thought to be mediated by infiltrating inflammatory cells [11,12]. CTX has been widely used in a large number of mouse HO models, such as the BMP-4 overexpression HO model [13,14], constitutively active activin receptor-like kinase-2 (caALK2) HO model [15—18], spinal cord injury neurogenic HO model [19], plasminogen deficiency HO model [20] and burn injury HO model [21]. Similar to human HO conditions, muscle injury seems to be indispensable for HO development in these experimental animal models. However, given the importance of muscle injury in HO pathogenesis, it is striking that few studies have justified the usage of CTX and explained by which mechanisms CTX-induced muscle injury facilitates HO formation.

This study examines the underlying cellular and molecular mechanisms linking muscle injury to HO by using CTX to induce muscle injury in a BMP-2—induced HO mouse model. Members of the BMP family have been the most popular agents in the study of HO since the identification of BMPs as the biologically active component(s) responsible for the osteoinductive capacity of demineralized bone matrix. HO mouse models based on injection, implantation and overexpression of BMPs in muscle, although nonphysiological, still represent reproducible models for studying HO progression and the cellular origins of HO. Studies based on these models suggest a population of fibrogeinc/adipogenic progenitors (FAPs) residing within the skeletal muscle interstitium as the cell origin for HO formation [22,23]. Human counterpart to these progenitor cells was also found and was shown to be involved in the pathogenesis of HO [24—27]. Mesenchymal progenitor cells corresponding to this lineage can be isolated by enzymatic digestion *in vitro* and may share common origin and characteristics of cells previously named muscle-derived stromal cells (MDSCs) [28,29].

Here, we hypothesized that soluble, proosteogenesis factors present in damaged muscle tissue are able to push MDSCs towards osteoblastic differentiation to facilitate HO formation. In this study, we sought to identify the osteoinductive factors actively involved in this process and demonstrated that locally produced BMP-7 after muscle injury could be a key factor in facilitating HO formation.

Methods

In vivo induction of HO

Using a protocol approved by the Institutional Animal Care and Use Committee (Protocol No. 18032493), the calf muscle of the right leg of 8- to 12-week-old male C57BL/6 J mice (Jackson laboratory, Bar Harbor, ME, USA) (N = 4) were first injected with 50 μL of 10 μM CTX (Calbiochem, San Diego, CA, USA). One day later, the calf muscles of both legs were injected with 0.5 μg of BMP-2 (R&D Systems, Minneapolis, MN, USA) encapsulated in 50 μL of photocrosslinked methacrylated 8% (w/v) gelatin hydrogel scaffold [30]. Two weeks later, mice were euthanized for imaging by micro—compute tomography (microCT) (vivaCT 40; Scanco Medical, Brüttisellen, Switzerland) to detect HO formation. Scans were acquired at 45 kVp, 88 μA, 300 ms integration time and at an isotropic voxel size of 35 μm. Region of volume was selected by including the whole length of the calf muscle, and region of interest was selected by drawing contour at each two-dimensional (2D) slice. Specifically, contours were drawn to include the opaque area of HO but to exclude the tibia and fibula areas. HO was defined by setting threshold to 212—1000. Bone density was calculated as mg hydroxyapatite (HA)/volume (cubic centimetre, ccm).

A separate group of mice (N = 4) were subcutaneously injected with 1 mg/kg dexamethasone daily (Vedco Inc., Saint Joseph, MO, USA) for seven days after CTX and BMP-2 injection to suppress inflammation. Two weeks later, mice were euthanized for microCT analysis of HO formation.

CTX-injured muscle tissue sample collection

Sample collection for CTX injection—alone group was performed as follows. The calf muscles of both legs of C57BL/6 J mice were injected with CTX as described earlier. At Day 3, Day 7 and Day 14 time points, mice were sacrificed and calf muscles from left and right sides were immediately harvested and snap-frozen in liquid nitrogen for later muscle tissue RNA and protein isolation, respectively. Uninjected mice served as Day 0 control (N = 3 for each time point).

A separate group of mice were used for muscle tissue—derived conditioned medium (CM) collection. The calf muscle of the right leg of C57 BL/6 J mice was injected with CTX as described earlier. On Day 2, mice were sacrificed and the calf muscles of both legs were processed as follows. Briefly, pooled muscle tissue samples (1 g) from either the control left leg or the CTX-injured right leg were cut into 3-mm pieces and cultured in 10 mL of growth medium [GM, high-glucose Dulbecco's Modified Eagle's Medium (Gibco, Gaithersburg, MD, USA) supplemented with 20% foetal bovine serum (Gemini Bio Products, West Sacramento, CA, USA) and 1% penicillin/streptomycin (Gibco)]. CM was changed and collected every day for three days and stored at −80 °C for later use.

In vitro osteogenesis induction with muscle tissue—derived CM

CM (N = 3) derived from CTX-injured muscle tissue (CTX CM) and CM derived from control muscle tissue (CTL CM) were used to culture MDSCs at a dilution of 1:2 in GM for three days. MDSCs (N = 3) were harvested from another cohort of mice according to a previously described protocol [28]. On culture Day 3, MDSCs were collected either for quantitative real-time reverse-transcription polymerase chain reaction analysis or Western blot analysis. PCR data and Western blot data were normalized to MDSCs cultured in GM only.

For inhibition of BMP-7 *in vitro* (N = 3), MDSCs were maintained for three days in GM or muscle tissue—derived CM with the supplementation of either 1 μg/mL of BMP-7—neutralizing antibody (ab27569; Abcam, Cambridge, MA, USA) or 1 μg/mL of isotype control antibody (ab171870; Abcam). On culture Day 3, MDSCs were collected for measurement of either alkaline phosphatase activity using an Alkaline Phosphatase Assay kit (ab83369; Abcam) or phosphorylated Smad1 level using a SMAD1 (pS463/S465) ELISA Kit (ab186036; Abcam). For the phosphorylated Smad1 ELISA, protein was extracted 1 h after the change of Day 3 CM.

Quantitative real-time reverse-transcription polymerase chain reaction analysis

Tissues or cells were lysed in QIAzol Lysis Reagent and isolated using the RNeasy Mini Kit according to the manufacturer's instructions (QIAGEN, Hilden, Germany). RNA was then converted to cDNA using the SuperScript IV First-Strand Synthesis System (Invitrogen, Carlsbad, CA, USA). Quantitative real-time PCR was performed with a StepOne Plus Real-Time PCR system using PowerUp SYBR Green Master Mix (Applied Biosystems, Foster City, CA, USA). The relative level of gene expression was calculated using the 2-delta delta Ct method. Primer sequences for actin, runt-related transcription factor 2 (*Runx2*), osterix (*OSX*), alkaline phosphatase (*ALP*), bone sialoprotein I (*BSP-1*), *BMPRIA*, *BMPRIB* and *ACVR1* are listed in Table 1.

Western blot

Total protein from tissues or cells was extracted using lysis buffer provided in the phosphorylated Smad1 ELISA kit. Protein concentration was determined using the bicinchoninic acid assay (ThermoFisher Scientific, Waltham, MA, USA), and equal loads of reduced protein samples were electrophoretically separated on NuPAGE 4—12% Bis-Tris Gel (Invitrogen) and then transferred to a polyvinylidene difluoride (PVDF) membrane using the iBlot Dry Blotting System (Invitrogen). Primary antibodies directed against BMP-2 (ab14933; Abcam), BMP-4 (ab39973; Abcam), BMP-7 (ab56023; Abcam), BMP-9 (ab35088; Abcam), glyceraldehyde-3-phosphate dehydrogenase (GAPDH) (CST5174; Cell Signaling Technology, Danvers, MA, USA), total Smad1 (CST6944; Cell Signaling Technology) and phosphorylated Smad1/5 (CST9516; Cell Signaling Technology) were incubated at 4 °C overnight, followed by horseradish peroxidase—conjugated secondary antibody (GE Healthcare Life Sciences, Marlborough, MA, USA) incubation. Western blots were developed using SuperSignal West Dura Extended Duration Substrate (ThermoFisher Scientific) and visualized using a FOTO/Analyst 1 Fx CCD imaging system (Fotodyne, Hartland, WI, USA).

Histology and immunostaining

Muscle tissues were fixed in methanol and embedded in paraffin. For histology, sections (9 μm thick) were collected on Colorfrost Plus Microscope Slides (ThermoFisher Scientific) and rehydrated, and hematoxylin and eosin (H&E) staining was performed according to a routine Harris Hematoxylin and Eosin protocol. Immunohistochemistry (IHC) was performed according to protocols described for the Vectastain Elite ABC Kit (Vector Laboratories Inc., Burlingame, CA, USA). Images were taken using a CKX41 microscope (Olympus, Tokyo, Japan) equipped with a DFC 3200 camera (Leica, Wetzlar, Germany). For immunofluorescence staining, tissue sections were blocked in 10% bovine serum albumin for 20 min and then incubated overnight at 4 °C with mixed primary antibodies against BMP-7 (ab56023; Abcam) and CD68 (ab53444; Abcam). On the second day, sections were incubated with mixed secondary antibodies against rabbit IgG (ab150077; Abcam) and rat IgG (ab150158; Abcam) at room temperature for 1 h. After washing, the slides were mounted with 4′,6-diamidino-2-phenylindole (DAPI)-containing mounting medium (Vector Laboratories). Slides were viewed using an inverted IX81 microscope (Olympus) equipped with a Retiga EXi cooled

Table 1 PCR primer sequences.

Genes	Forward (5′ to 3′)	Reverse (5′ to 3′)
Actin	GGCTGTATTCCCCTCCATCG	CCAGTTGGTAACAATGCCATGT
Runx2	ATGATGACACTGCCACCTCTGAC	ACTGCCTGGGGTCTGAAAAAGG
OSX	GATGGCGTCCTCTCTGCTT	CGTATGGCTTCTTTGTGCCT
ALP	ATCGGAACAACCTGACTGACCCTT	ACCCTCATGATGTCCGTGGTCAAT
BSP-1	TGCCCTCTGATCAGGACAAC	ATCCGACTGATCGGCACTCT
BMPRIA	ACCAGACGGTGTTAATGCGT	CTCGATGAGCAATTGCAGGC
BMPRIB	CCCTCGGCCCAAGATCCTA	CAACAGGCATTCCAGAGTCATC
ACVR1	GTGGAAGATTACAAGCCACCA	GGGTCTGAGAACCATCTGTTAGG

PCR = polymerase chain reaction.

CCD camera (Qimaging, Surrey, BC, Canada) and MetaMorph software (Molecular Devices, San Jose, CA, USA).

Inhibition of BMP-7 *in vivo*

The calf muscle of the right leg of C57 BL/6 J mice was injected with CTX as described earlier. One day later, the calf muscles of both legs were injected with 0.5 μg of BMP-2 (R&D Systems) either with 5 μg of BMP-7—neutralizing antibody (ab27569; Abcam) ($N = 4$) or 5 μg of isotype control antibody (ab171870; Abcam) ($N = 4$) coencapsulated in 50 μL of photocrosslinked methacrylated 8% (w/v) gelatin hydrogel scaffold. Two weeks later, mice were euthanized for imaging by microCT to detect the change in HO volume. Same scan setting was used as previously described.

Statistical analysis

All data were expressed as mean ± standard deviation. Student *t* test was used to make comparisons between two groups, while one-way analysis of variance followed by the Tukey multiple comparisons test was used for comparisons of three or more groups. Statistical significance (*) was considered at $p < 0.05$. Statistical analyses were performed using GraphPad Prism 7.0 software (GraphPad Software Inc., La Jolla, CA, USA).

Results

CTX-induced muscle injury significantly increased HO volume

To determine the role of muscle injury in HO formation, CTX was injected into the calf muscle of the right leg of the animal one day before BMP-2 injection into the calf muscles of both legs. Two weeks later, microCT imaging and analysis showed significantly larger bone volume in the right legs that were coinjected with CTX and BMP-2 (3.458 ± 0.994 mm^3), than in the left legs that were injected with BMP-2 alone (1.573 ± 0.577 mm^3) ($p = 0.0168$) (Fig. 1A). Histology revealed severe inflammatory cell infiltration into the muscle tissue of the CTX-injured leg, while such infiltration was absent in the group with BMP-2 injection alone (Fig. 1B). Bone tissue became evident after two weeks when most of the hydrogel vehicle had been degraded. There were no morphological differences (Supplemental Fig. 1) between the bone formed in the different groups and no qualitative differences in bone mineral density ($p = 0.1493$) (Fig. 1A).

CTX-induced muscle injury generated an osteoinductive environment with BMP signalling activation

CTX administration alone was not sufficient for the induction of HO, and the inflammatory response was resolved after two weeks (data not shown). However, during this regeneration process, BMP signalling was activated with significantly higher phosphorylated Smad1 level observed 7 days after muscle injury ($p = 0.0046$) (Fig. 2A). Osteogenic marker genes were also found to be upregulated with the expression of different genes peaking at different time points (*Runx2*, $p = 0.0202$; *BSP-1*, $p < 0.0001$; *OSX*, $p = 0.0022$) (Fig. 2B), suggesting the generation of a proosteogenesis environment with highly coordinated gene regulation after muscle injury.

To explore how this proosteogenesis environment could promote HO formation, muscle tissue—derived CM was collected and applied to MDSCs in culture. After exposure to either GM or CM for two days, MDSC cultures were extracted for total protein at various time points after the change of medium on Day 3. BMP signalling activation was observed immediately after the application of GM and CM (Fig. 2C). However, the phosphorylation of Smad1/5 protein level diminished in the GM group quickly but persisted in CM groups for an extended period of time. Phosphorylation of Smad1/5 protein level in CM groups peaked at the 1-h time point and remained the highest in the CTX CM treatment group thereafter (Fig. 2C). Exposure to CTX CM was also found to greatly enhance osteogenic marker gene expression in MDSCs compared with exposure to CTL CM (*OSX*, $p = 0.0328$; *ALP*, $p = 0.0240$; *BSP-1*, $p = 0.9301$) (Fig. 2D). Concomitantly, *BMPRIB* gene expression increased significantly in MDSCs cultured in CTX CM (*BMPRIA*, $p = 0.7269$; *BMPRIB*, $p = 0.0411$; *ACVR1*, $p = 0.6717$) (Fig. 2D). Taken together, these results suggested that soluble factor(s) present in injured muscle tissue were able to promote MDSC osteogenesis via BMP signalling pathway.

BMP-7 level increased in CTX-injured muscle

To identify the soluble factor(s) involved in BMP signalling activation, Western blotting was performed to examine the

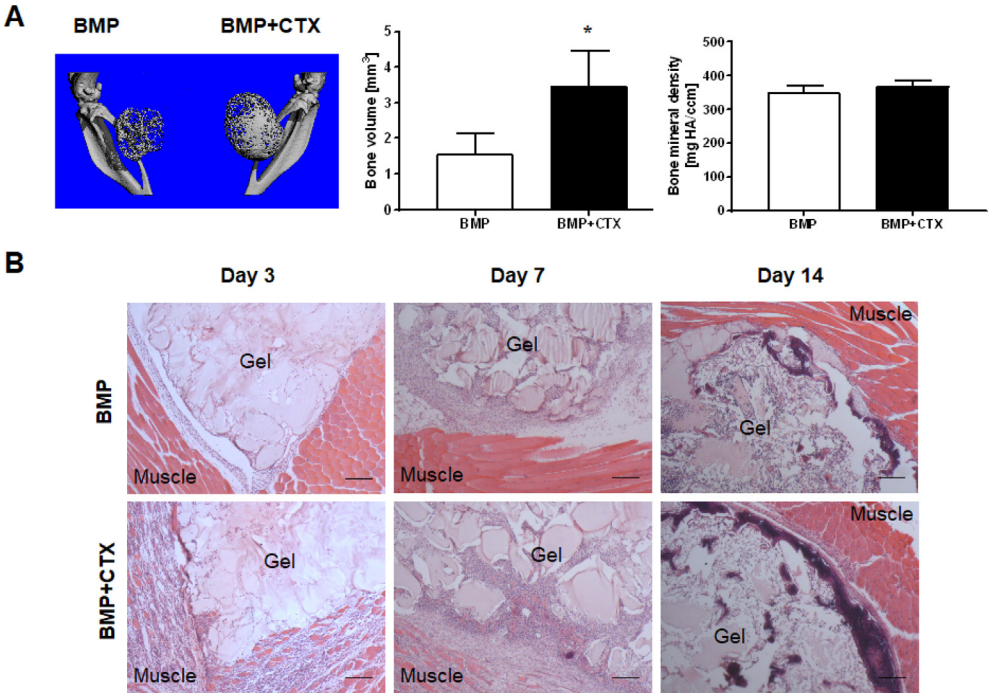

Figure 1 CTX-induced muscle injury significantly increased HO volume. (A) microCT imaging and analysis. Significantly larger HO volume was observed in the BMP-2/CTX coinjection group (right leg) compared with the group receiving BMP-2 injection alone (left leg) (*, $p < 0.05$; n = 4). No significant difference in bone mineral density was found between the two groups. **(B)** H&E staining illustrating the time course of HO progression. Severe inflammatory response in muscle tissue was seen at the early time points in the CTX-injured groups. Scale bar = 200 μm.
BMP-2 = bone morphogenetic protein-2; CTX = cardiotoxin; HO = heterotopic ossification; H&E = hematoxylin and eosin.

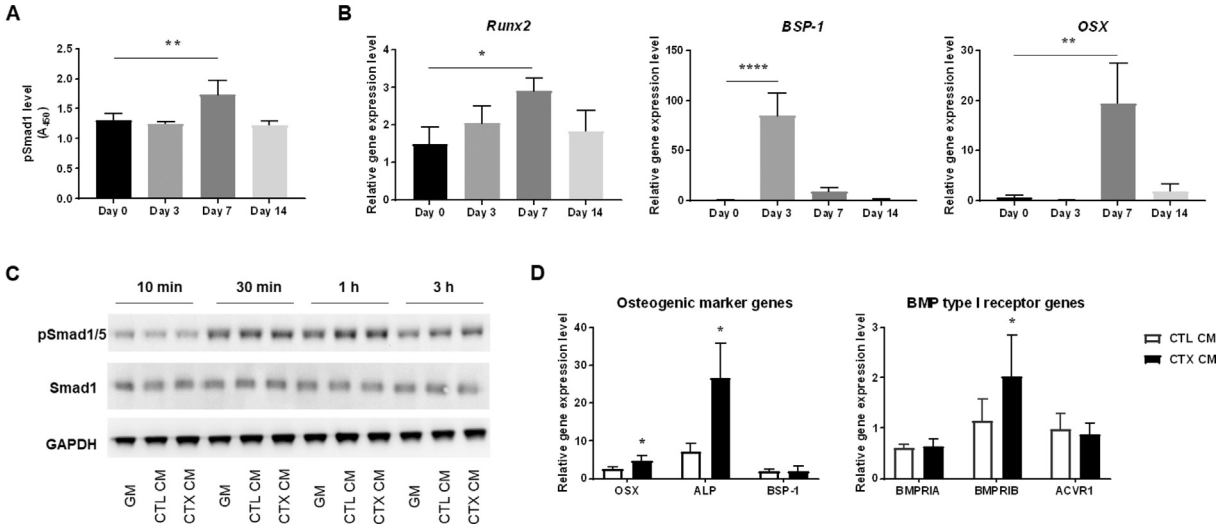

Figure 2 CTX-induced muscle injury generated an osteoinductive environment. (A) Phosphorylated Smad1 level in muscle tissue lysates measured by pSMAD1 ELISA at different time points after CTX injection demonstrated the activation of BMP signalling (**, $p < 0.01$; n = 3). **(B)** PCR analysis showed the upregulation of osteogenic marker gene expression in muscle tissue after CTX injection with the expression of different genes peaking at different time points. (*, $p < 0.05$; **, $p < 0.01$; ****, $p < 0.0001$; n = 3). Data are normalized to uninjected Day 0 control mice. **(C)** Western blot analysis of phosphorylated Smad1/5 protein and total Smad1 levels revealed the time course of BMP signalling activation in MDSCs cultured in GM and muscle tissue—derived CM. **(D)** PCR analysis of osteogenic marker gene and BMP type I receptor gene expression in MDSCs. Significantly higher *OSX*, *ALP* and *BMPR1B* expression was detected in MDSCs cultured in CTX CM compared with CTL CM (*, $p < 0.05$; n = 3). Data are normalized to MDSCs cultured in GM.
BMP = bone morphogenetic protein; CM = conditioned medium; CTX = cardiotoxin; CTL CM, CM derived from control muscle tissue; CTX CM, CM derived from CTX-injured muscle tissue; ELISA = enzyme-linked immunosorbent assay; GM = growth medium; MDSCs = muscle-derived stromal cells; PCR = polymerase chain reaction.

expression profile of several BMP ligands that have been reported to exhibit significant osteoinductive potential [31]. Among these BMP subtypes, we found that BMP-7 expression changed drastically with substantially increased expression 3 days after muscle injury, whereas BMP-2, BMP-4 and BMP-9 expression remained relatively constant during the muscle regeneration period (Fig. 3A). Histology confirmed the expression of BMP-7 on CTX-injured muscle tissue at 48 h after CTX injury, but not on control uninjured muscle tissue (Fig. 3B). Histology also revealed severe inflammatory cell infiltration into the muscle tissue, suggesting the possibility that BMP-7 could be derived from the infiltrating inflammatory cells. Double immunofluorescence staining indeed demonstrated the presence of the macrophage marker, CD68, localized in close proximity to BMP-7 signals (Fig. 3C). There were double positive cells and single positive cells for either marker in CTX-injured muscle tissue.

Inhibiting BMP-7 activity *in vitro* suppressed the osteogenesis-promoting effect of CM derived from CTX-injured muscle tissue

To assess the functional involvement of BMP-7, the effect of supplementing BMP-7—neutralizing antibody on muscle tissue CM was tested on the promotion of MDSC osteogenesis, based on ALP activity and phosphorylated Smad1 level. Our results showed that ALP activity increased significantly in MDSCs cultured in CTX CM compared with CTL CM ($p < 0.0001$) and that this osteogenesis-promoting effect of CTX CM was significantly inhibited in the presence of BMP-7—neutralizing antibody ($p = 0.0017$) (Fig. 4A). Concomitantly, addition of BMP-7—neutralizing antibody to CM resulted in the reduction of phosphorylated Smad1 to a nearly basal level (Fig. 4B), validating the functional involvement of BMP-7 in BMP signalling activation *in vitro*.

Inhibiting BMP-7 activity *in vivo* reduced HO volume

To assess the *in vivo* relevance of the *in vitro* findings, BMP-7—neutralizing antibody was coencapsulated in hydrogel scaffold at the time of BMP-2 injection in the mouse HO model. microCT imaging and analysis at two weeks showed significantly reduced bone volume in both legs of animals receiving BMP-7—neutralizing antibody treatment (left leg: 0.3715 ± 0.1016 mm^3; right leg: 1.642 ± 0.5055 mm^3) compared with animals receiving isotype control antibody treatment (left leg: 1.557 ± 0.4149 mm^3; right leg: 3.875 ± 0.6129 mm^3) (left leg: $p = 0.0332$; right leg: $p = 0.0365$) (Fig. 4C). No qualitative differences in bone

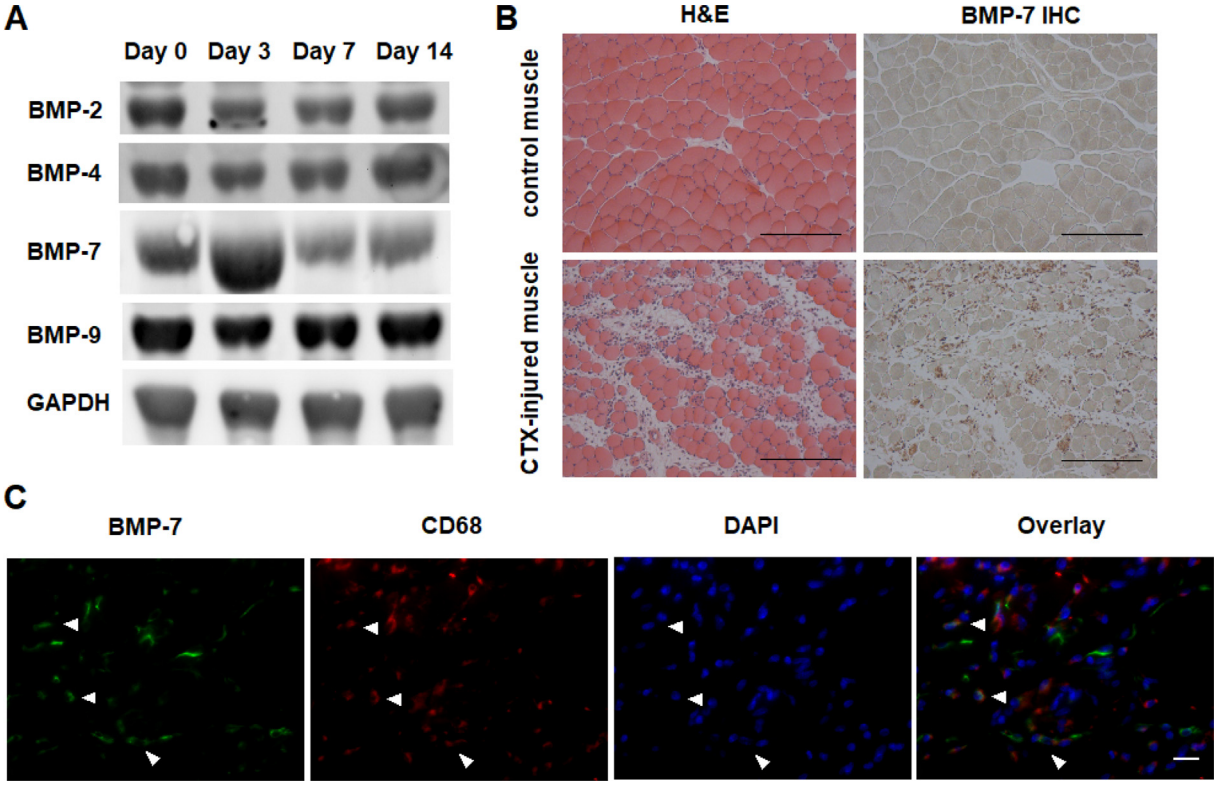

Figure 3 BMP-7 level increased in CTX-injured muscle. (A) Western blot analysis of the expression profile of selected BMP ligands after muscle injury. **(B)** H&E and IHC images showing the presence and distribution of BMP-7 in CTX-injured muscle tissue at 48 h after CTX injury. Bar = 200 μm. **(C)** Immunofluorescence staining showing the location of BMP-7 (green) in relation to macrophage marker CD68 (red) in CTX-injured muscle tissue. Arrowheads indicate the double positive cells present in CTX-injured muscle tissue. Bar = 20 μm.
BMP = bone morphogenetic protein; CTX = cardiotoxin; H&E = hematoxylin and eosin; IHC = immunohistochemistry.

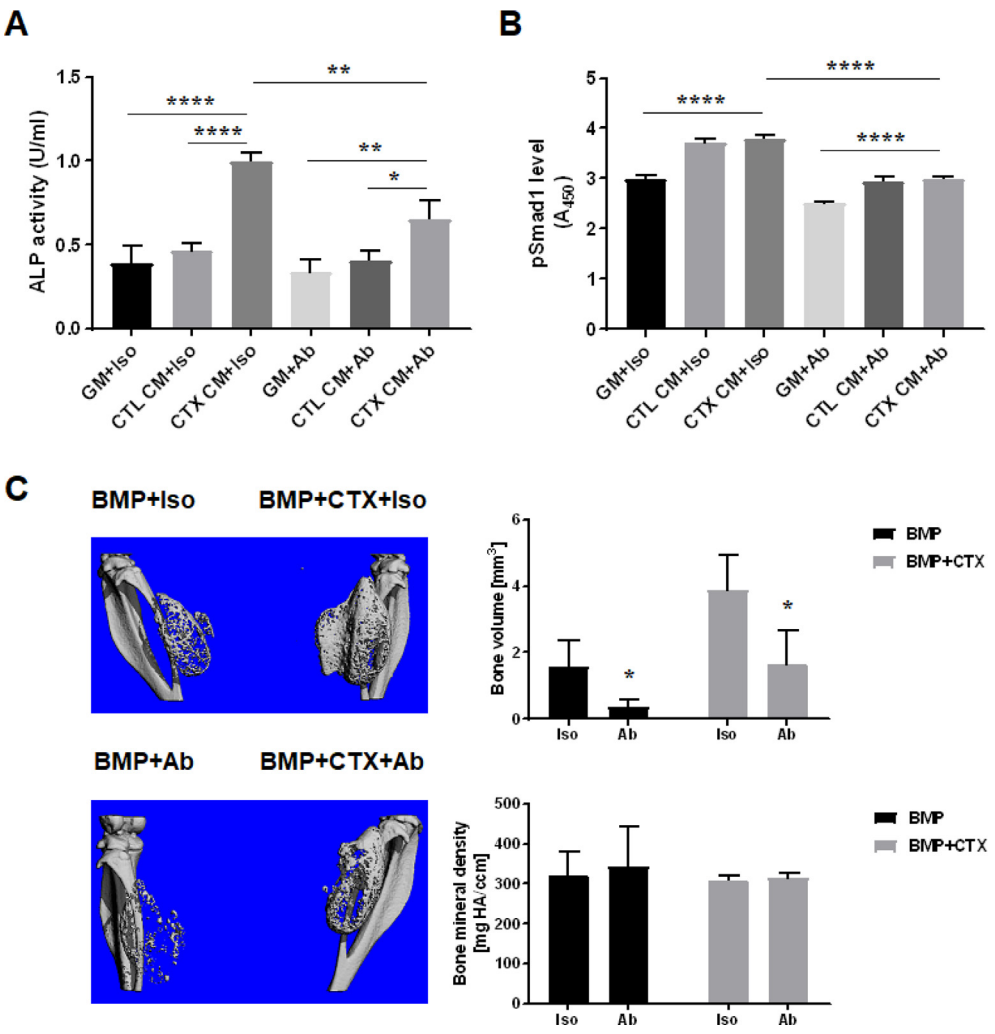

Figure 4 Inhibition of BMP-7 activity suppressed osteogenesis *in vitro* and reduced HO formation *in vivo*. (A) Osteogenesis of MDSCs *in vitro*. ALP activity measured in different groups of cell lysates showed that treatment with BMP-7—neutralizing antibody suppressed the osteogenesis-promoting effect of CTX CM (*, $p < 0.05$; **, $p < 0.01$; ****, $p < 0.0001$; n = 3). Iso: isotype control antibody treatment group; Ab: BMP-7—neutralizing antibody treatment group. **(B)** BMP signalling *in vitro*. Phosphorylated Smad1 level in cell lysates measured by pSMAD1 ELISA showed that activation of BMP signalling was inhibited with addition of BMP-7—neutralizing antibody (****, $p < 0.0001$; n = 3). **(C)** HO formation *in vivo*. microCT imaging and analysis showed significant reduction in HO volume upon BMP-7—neutralizing antibody treatment compared with isotype control antibody treatment (*, $p < 0.05$; n = 4). No significant difference in bone mineral density was found between BMP-7—neutralizing antibody and isotype control antibody treatment groups. ALP = alkaline phosphatase; BMP = bone morphogenetic protein; CM = conditioned medium; CTX = cardiotoxin; CTL CM, CM derived from control muscle tissue; CTX CM, CM derived from CTX-injured muscle tissue; ELISA = enzyme-linked immunosorbent assay; GM = growth medium; HO = heterotopic ossification; MDSCs = muscle-derived stromal cells; microCT = micro—computed tomography.

mineral density were found between BMP-7—neutralizing antibody and isotype control antibody treatment groups (left leg: $p = 0.7326$; right leg: $p = 0.6567$) (Fig. 4C).

Suppression of inflammation reduced HO volume with concomitant reduction of BMP-7 production in CTX-injured muscle

To assess the involvement of inflammation in HO formation, the antiinflammatory drug, dexamethasone, was administered to the animals for 7 days to suppress the inflammatory response induced by muscle injury. microCT imaging and analysis at two weeks showed significantly reduced bone volume in both legs (left leg: 0.0803 ± 0.119 mm^3; right leg: 0.717 ± 0.396 mm^3) (Fig. 5A) compared with animals that did not receive antiinflammatory drug treatment (left leg: 1.573 ± 0.577 mm^3; right leg: 3.458 ± 0.994 mm^3) (Fig. 1A) (left leg: $p = 0.0023$; right leg: $p = 0.0022$). Histological observation showed that with dexamethasone administration, severe inflammatory cell infiltration into damaged muscle tissue was no longer evident in CTX-injured legs at the early time points (Fig. 5B). In addition, the HO formed was less mineralized in both legs after dexamethasone treatment (left leg: 219.2 ± 44.94 mg HA/ccm; right leg: 296.8 ± 8.453 mg HA/ccm) (Fig. 5A) than in animals that did not receive antiinflammatory drug treatment (left leg: 348.1 ± 10.45 mg HA/ccm; right leg:

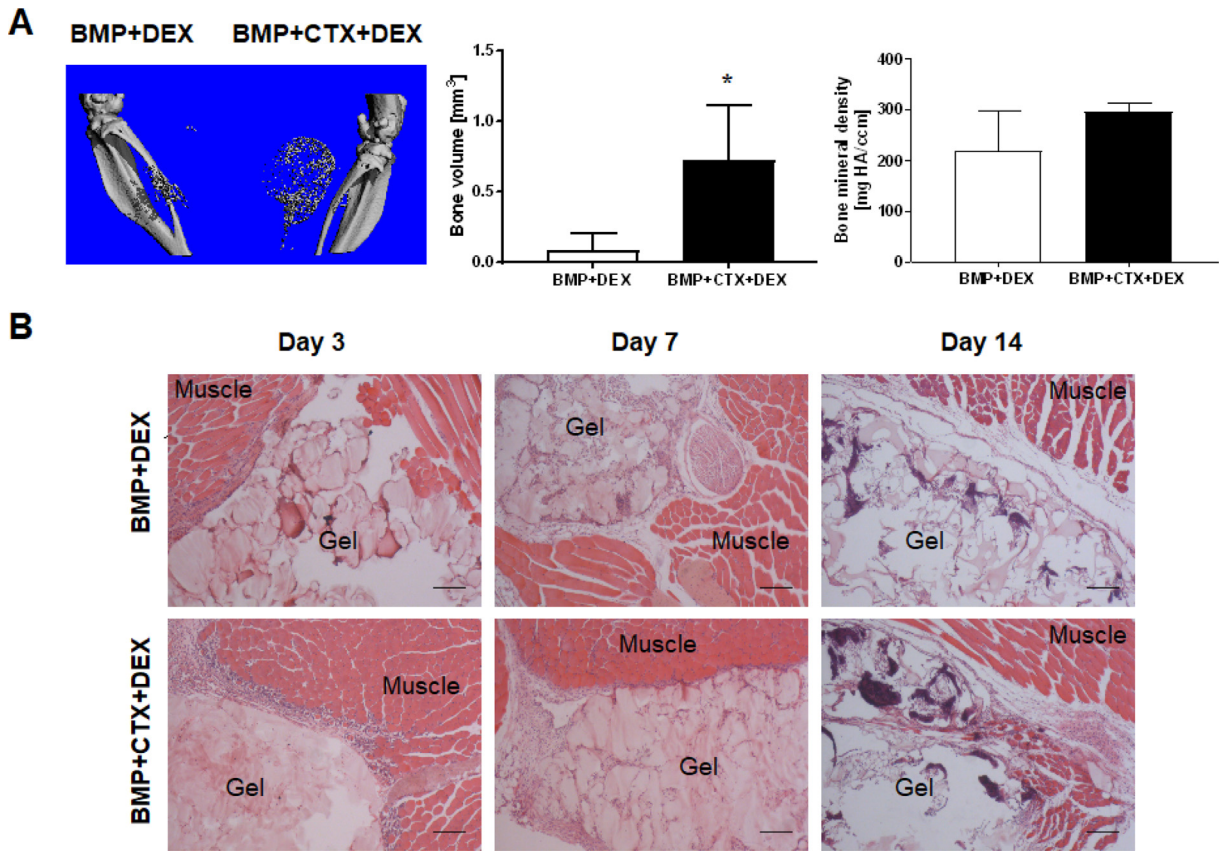

Figure 5 Suppression of inflammation reduced HO volume *in vivo*. (A) microCT imaging and analysis. Reduction of HO volume and bone mineral density was observed in animals treated with the antiinflammatory drug dexamethasone (DEX) (*, $p < 0.05$; n = 4). **(B)** H&E staining illustrating the time course of HO progression in animals treated with antiinflammatory drug. A diminished inflammatory response was found in CTX-injured muscle. Bar = 200 μm.
CTX = cardiotoxin; H&E = hematoxylin and eosin; HO = heterotopic ossification; microCT = micro—computed tomography.

370 ± 8.133 mg HA/ccm) (Fig. 1A) (left leg: $p = 0.0225$; right leg: $p = 0.0017$).

Immunofluorescence staining showed decreased CD68-positive macrophage numbers in CTX-injured muscle of dexamethasone-treated animals compared with animals without dexamethasone treatment, at both the Day 3 and Day 7 time points (Day 3: $p = 0.0027$; Day 7: $p = 0.0099$) (Fig. 6). Importantly, in addition to decreased macrophage number in the dexamethasone-treated group, BMP-7 level in CTX-injured muscle tissue was also greatly reduced at the Day 3 time point ($p = 0.0111$) (Fig. 6A&B). BMP-7 expression was only detectable within 3 days after CTX injury and was undetectable beyond the acute inflammatory phase (Fig. 6A&C).

Discussion

In this study, we first set out to determine the role of muscle injury in HO formation by using CTX to induce muscle injury in a BMP-2—induced HO mouse model. Our results showed that CTX-induced muscle injury significantly increased the volume of BMP-2-induced HO (Fig. 1A) together with increased osteogenic marker gene expression (Fig. 2B) and increased level of phosphorylated Smad1 (Fig. 2A), suggesting the generation of a proosteogenesis environment after CTX treatment.

Then, we sought to explore by which mechanism muscle injury facilitates HO formation. To test the possibility that soluble factors present in damaged muscle tissue have an osteogenesis-promoting effect, we compared the effect of exposing MDSCs to culture medium conditioned by explanted control muscle tissue (CTL CM) *versus* those conditioned by explanted CTX-injured muscle tissue (CTX CM). MDSCs are likely the same cell type identified as the muscle interstitial—resident FAPs previously found to mediate BMP-2—induced HO *in vivo* [22,23]. The MDSCs used in this study are positive for the surface markers Sca-1 and PDGFRα, have strong osteogenic potential and are highly responsive to BMP signal *in vitro* (Supplemental Fig. 2). Our data showed that CTX CM is capable of promoting osteogenesis by upregulating osteogenic marker gene and BMP receptor gene expression in MDSCs (Fig. 2D) along with BMP signalling activation (Fig. 2C), suggesting that certain BMP family proteins are present in the damaged muscle milieu and are capable of exerting an osteogenesis-promoting effect on MDSCs. Notably, we also found that CTL CM is also capable of promoting MDSCs osteogenesis and activates BMP signalling compared with GM, but to a lesser extent than CTX CM. We speculate that this is because either certain

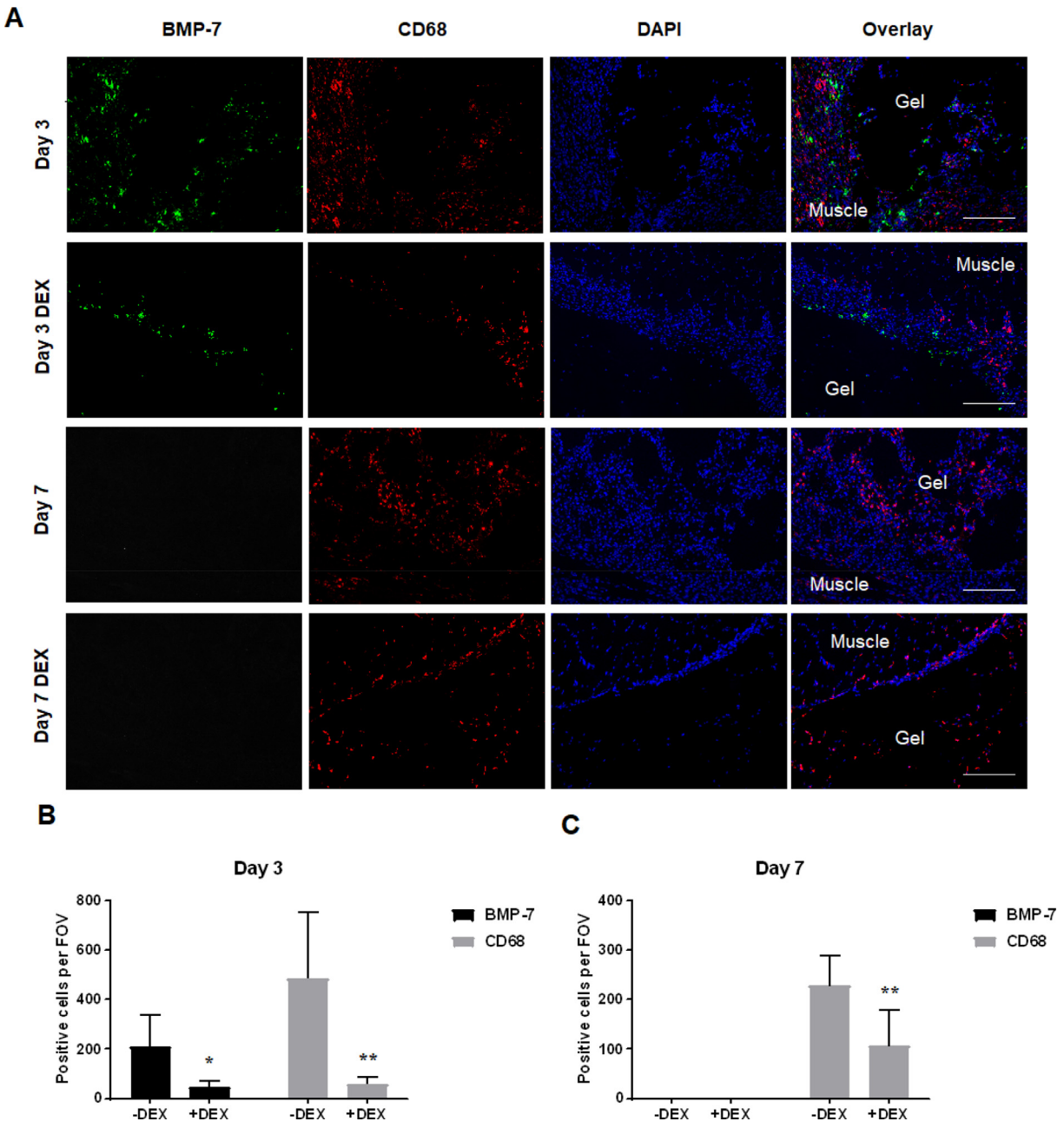

Figure 6 Suppression of inflammation *in vivo* reduced BMP-7 level in CTX-injured muscle. (A) Immunofluorescence staining showing decreased macrophage number (CD68, red) and reduced BMP-7 level (green) in CTX-injured muscle in animals treated with the antiinflammatory drug dexamethasone (DEX). Bar = 200 μm. **(B and C)** Quantitative analysis of BMP-7+ and CD68 + cells at the interface of hydrogel scaffold and muscle. BMP-7+ and CD68 + cells were counted on 6 independent fields of view (FOV, 20 × magnification). **(B)** On Day 3, significant decrease in the number of BMP-7+ and CD68 + cells was observed in dexamethasone-treated animals (*, $p < 0.05$; **, $p < 0.01$). **(C)** On Day 7, significant decrease in the number of CD68 + cells was observed in dexamethasone-treated animals (**, $p < 0.01$), while BMP-7+ cells were not detected.
BMP-7 = bone morphogenetic protein-7; CTX = cardiotoxin.

proosteogenesis factors are present at basal level in uninjured muscle tissue or the muscle tissue was unavoidably injured during its collection process resulting from incision and cutting. In summary, our findings suggest a general mechanism by which muscle injury facilitates HO formation via the soluble factors present in injured muscle that act to induce MDSC osteogenesis through BMP signalling pathway.

To identify which soluble factor is responsible for BMP signalling activation after muscle injury, Western blotting was performed against selected BMP subtypes that have been reported with great osteoinductive potential. We found that BMP-7 expression was highly upregulated at early time points after muscle injury and that its expression was localized only to inflamed areas of muscle tissue highly

populated by CD68-positive macrophages (Fig. 3). We did not observe the change in expression of other BMP subtypes in injured muscle tissue. As ligand specificity of BMP signalling is mainly dictated by BMP type I receptor, with BMP-2/BMP-4 having a higher affinity for BMPRIA and BMP-6/BMP-7 for BMPRIB [32], the upregulation of BMP-7 was consistent with our *in vitro* finding that among the BMP type I receptors, only *BMPRIB* expression was significantly upregulated in MDSCs after being exposed to muscle tissue CM (Fig. 2D). To confirm the functional involvement of BMP-7, we performed BMP-7 inhibition experiment both *in vitro* and *in vivo*. Treatment with BMP-7—neutralizing antibody significantly inhibited the osteogenesis-promoting effect of CTX CM *in vitro* and reduced HO volume *in vivo* (Fig. 4), strongly implicating the role of BMP-7 as a key osteoinductive factor responsible for the osteogenesis-promoting effect of muscle injury.

BMP-7, also known as osteogenic protein-1, is a Food and drug Administration—approved osteoinductive adjuvant in orthopaedic surgery known for its role in triggering stem cell osteogenic differentiation [33]. However, the physiological role of BMP-7 after muscle injury and its cellular origin are not clear at this point. Previous studies have shown that BMP signalling is normally active in muscle and important in maintaining muscle mass and that inhibition of BMP signalling leads to muscle atrophy [34,35]. Studies have also shown that BMP signalling is indispensable for muscle regeneration after injury and that BMP signalling activation coincides with the period of satellite cell proliferation [36]. Therefore, BMP-7 may function to promote satellite cell proliferation in injured muscle [37,38]. Recently, it has become clear that BMP-7 is a highly pleiotropic factor [39]. For example, it has been reported that BMP-7 inhibits inflammation by inducing M2 macrophage differentiation [40]. It can also act as an antifibrotic cytokine by antagonizing transforming growth factor-β1 (TGF-β1) [41—43]. Given the close spatial proximity of BMP-7 signal and macrophage signal observed by immunofluorescence staining, the upregulation of BMP-7 in injured muscle may also be a mechanism to counteract muscle injury—induced inflammation and fibrosis. However, in pathological conditions, such as in our case with supraphysiological dose of BMP-2, this otherwise physiological BMP-7 signal may well turn into strong osteogenic signal to cause aberrant osteogenesis.

Finally, we showed that antiinflammatory drug treatment reduced the volume of HO formation *in vivo*, with evident decreases in inflammatory cell infiltration (Fig. 5). In addition, we found decreased BMP-7 level in CTX-injured muscle tissue in dexamethasone-treated animals compared with those not receiving the drug (Fig. 6). The positive correlation between BMP-7 levels and macrophage numbers suggests that the osteogenesis-promoting effect of muscle injury could be largely related to the injury-induced inflammatory response. Our results thus provide a possible rationale for using antiinflammatory drugs as HO prevention. Interestingly, we also observed in our study that either inhibition of BMP-7 activity or suppression of inflammation reduced the volume of HO in the left legs subjected only to BMP-2 injection. This can be explained by the fact that recombinant BMP triggers dose-dependent inflammatory reactions *in vivo* [44], and hydrogel muscle injection may cause mild muscle tissue injury. Indeed, we observed BMP-7 expression located at the interface of BMP-2 hydrogel and muscle in the BMP-2 injection—alone group, which became even less evident in animals receiving antiinflammatory drug treatment (Supplemental Fig. 3).

The limitation of this study is that the role of other types of muscle injury in HO pathogenesis was not tested. It is possible that other factors are responsible for the osteogenesis-promoting effect of distinct types of muscle injury or more than one factor may function at different time points after injury. Of particular relevance is a study that demonstrated the presence of BMP-4 ligand in human blast traumatized skeletal muscle tissue [45]. However, we did not find upregulation of BMP-4 in our system. This may be due to different injury mechanism, tissue harvest time and differences between human and mouse. In summary, our results demonstrate that CTX-induced muscle injury augments BMP-2—induced HO formation by stimulating local BMP-7 production and that this osteogenesis-promoting effect is largely related to the muscle injury—induced inflammatory response. Our findings suggest a universal mechanism by which muscle injury facilitates HO formation.

Funding information

This study was supported by Commonwealth of Pennsylvania Department of Health (SAP4100062224, SAP4100050913) and China Scholarship Council (awarded to L.L.).

Conflict of interest

There is no conflict of interest to disclose.

Acknowledgements

The authors thank Dr Hongshuai Li (University of Pittsburgh) for assistance with the microCT analyses, Alyssa Falcione (University of Pittsburgh) for advice regarding animal medication treatments and Dr Peter Mittwede (University of Pittsburgh) for manuscript editing.

Appendix A. Supplementary data

Supplementary data to this article can be found online at https://doi.org/10.1016/j.jot.2019.06.001.

References

[1] Shehab D, Elgazzar AH, Collier BD. Heterotopic ossification. J Nucl Med 2002;43(3):346—53.
[2] Shore EM, Xu M, Feldman GJ, Fenstermacher DA, Cho TJ, Choi IH, et al. A recurrent mutation in the BMP type I receptor ACVR1 causes inherited and sporadic fibrodysplasia ossificans progressiva. Nat Genet 2006;38(5):525—7.
[3] McCarthy EF, Sundaram M. Heterotopic ossification: a review. Skeletal Radiol 2005;34(10):609—19.
[4] Pignolo RJ, Shore EM, Kaplan FS. Fibrodysplasia ossificans progressiva: clinical and genetic aspects. Orphanet J Rare Dis 2011;6:80.

[5] van Kuijk AA, Geurts AC, van Kuppevelt HJ. Neurogenic heterotopic ossification in spinal cord injury. Spinal Cord 2002; 40(7):313—26.
[6] Anthonissen J, Ossendorf C, Hock JL, Steffen CT, Goetz H, Hofmann A, et al. The role of muscular trauma in the development of heterotopic ossification after hip surgery: an animal-model study in rats. Injury 2016;47(3):613—6.
[7] Forsberg JA, Pepek JM, Wagner S, Wilson K, Flint J, Andersen RC, et al. Heterotopic ossification in high-energy wartime extremity injuries: prevalence and risk factors. J Bone Joint Surg Am 2009;91(5):1084—91.
[8] Balboni TA, Gobezie R, Mamon HJ. Heterotopic ossification: pathophysiology, clinical features, and the role of radiotherapy for prophylaxis. Int J Radiat Oncol Biol Phys 2006; 65(5):1289—99.
[9] Huang H, Cheng WX, Hu YP, Chen JH, Zheng ZT, Zhang P. Relationship between heterotopic ossification and traumatic brain injury: why severe traumatic brain injury increases the risk of heterotopic ossification. J Orthop Translat 2018;12: 16—25.
[10] Kumar TK, Jayaraman G, Lee CS, Arunkumar AI, Sivaraman T, Samuel D, et al. Snake venom cardiotoxins-structure, dynamics, function and folding. J Biomol Struct Dyn 1997;15(3): 431—63.
[11] Arnold L, Henry A, Poron F, Baba-Amer Y, van Rooijen N, Plonquet A, et al. Inflammatory monocytes recruited after skeletal muscle injury switch into antiinflammatory macrophages to support myogenesis. J Exp Med 2007;204(5): 1057—69.
[12] Yang W, Hu P. Skeletal muscle regeneration is modulated by inflammation. J Orthop Translat 2018;13:25—32.
[13] Kan L, Liu Y, McGuire TL, Berger DM, Awatramani RB, Dymecki SM, et al. Dysregulation of local stem/progenitor cells as a common cellular mechanism for heterotopic ossification. Stem Cell 2009;27(1):150—6.
[14] Lounev VY, Ramachandran R, Wosczyna MN, Yamamoto M, Maidment AD, Shore EM, et al. Identification of progenitor cells that contribute to heterotopic skeletogenesis. J Bone Joint Surg Am 2009;91(3):652—63.
[15] Kan L, Lounev VY, Pignolo RJ, Duan L, Liu Y, Stock SR, et al. Substance P signaling mediates BMP-dependent heterotopic ossification. J Cell Biochem 2011;112(10):2759—72.
[16] Chakkalakal SA, Zhang D, Culbert AL, Convente MR, Caron RJ, Wright AC, et al. An Acvr1 R206H knock-in mouse has fibrodysplasia ossificans progressiva. J Bone Miner Res 2012;27(8): 1746—56.
[17] Agarwal S, Loder SJ, Cholok D, Peterson J, Li J, Breuler C, et al. Scleraxis-lineage cells contribute to ectopic bone formation in muscle and tendon. Stem Cell 2017;35(3):705—10.
[18] Dey D, Bagarova J, Hatsell SJ, Armstrong KA, Huang L, Ermann J, et al. Two tissue-resident progenitor lineages drive distinct phenotypes of heterotopic ossification. Sci Transl Med 2016;8(366). 366ra163.
[19] Genet F, Kulina I, Vaquette C, Torossian F, Millard S, Pettit AR, et al. Neurological heterotopic ossification following spinal cord injury is triggered by macrophage-mediated inflammation in muscle. J Pathol 2015;236(2):229—40.
[20] Mignemi NA, Yuasa M, Baker CE, Moore SN, Ihejirika RC, Oelsner WK, et al. Plasmin prevents dystrophic calcification after muscle injury. J Bone Miner Res 2017;32(2):294—308.
[21] Moore SN, Hawley GD, Smith EN, Mignemi NA, Ihejirika RC, Yuasa M, et al. Validation of a radiography-based quantification designed to longitudinally monitor soft tissue calcification in skeletal muscle. PLoS One 2016;11(7):e0159624.
[22] Joe AW, Yi L, Natarajan A, Le Grand F, So L, Wang J, et al. Muscle injury activates resident fibro/adipogenic progenitors that facilitate myogenesis. Nat Cell Biol 2010; 12(2):153—63.
[23] Wosczyna MN, Biswas AA, Cogswell CA, Goldhamer DJ. Multipotent progenitors resident in the skeletal muscle interstitium exhibit robust BMP-dependent osteogenic activity and mediate heterotopic ossification. J Bone Miner Res 2012;27(5): 1004—17.
[24] Uezumi A, Fukada S, Yamamoto N, Ikemoto-Uezumi M, Nakatani M, Morita M, et al. Identification and characterization of PDGFRalpha+ mesenchymal progenitors in human skeletal muscle. Cell Death Dis 2014;5:e1186.
[25] Jackson WM, Aragon AB, Bulken-Hoover JD, Nesti LJ, Tuan RS. Putative heterotopic ossification progenitor cells derived from traumatized muscle. J Orthop Res 2009;27(12):1645—51.
[26] Davis TA, O'Brien FP, Anam K, Grijalva S, Potter BK, Elster EA. Heterotopic ossification in complex orthopaedic combat wounds: quantification and characterization of osteogenic precursor cell activity in traumatized muscle. J Bone Joint Surg Am 2011;93(12):1122—31.
[27] Torossian F, Guerton B, Anginot A, Alexander KA, Desterke C, Soave S, et al. Macrophage-derived oncostatin M contributes to human and mouse neurogenic heterotopic ossifications. JCI Insight 2017;2(21).
[28] Glass GE, Chan JK, Freidin A, Feldmann M, Horwood NJ, Nanchahal J. TNF-alpha promotes fracture repair by augmenting the recruitment and differentiation of muscle-derived stromal cells. Proc Natl Acad Sci U S A 2011;108(4): 1585—90.
[29] Leblanc E, Trensz F, Haroun S, Drouin G, Bergeron E, Penton CM, et al. BMP-9-induced muscle heterotopic ossification requires changes to the skeletal muscle microenvironment. J Bone Miner Res 2011;26(6):1166—77.
[30] Lin H, Cheng AW, Alexander PG, Beck AM, Tuan RS. Cartilage tissue engineering application of injectable gelatin hydrogel with in situ visible-light-activated gelation capability in both air and aqueous solution. Tissue Eng 2014;20(17—18): 2402—11.
[31] Luu HH, Song WX, Luo X, Manning D, Luo J, Deng ZL, et al. Distinct roles of bone morphogenetic proteins in osteogenic differentiation of mesenchymal stem cells. J Orthop Res 2007; 25(5):665—77.
[32] ten Dijke P, Yamashita H, Sampath TK, Reddi AH, Estevez M, Riddle DL, et al. Identification of type I receptors for osteogenic protein-1 and bone morphogenetic protein-4. J Biol Chem 1994;269(25):16985—8.
[33] Cecchi S, Bennet SJ, Arora M. Bone morphogenetic protein-7: review of signalling and efficacy in fracture healing. J Orthop Translat 2016;4:28—34.
[34] Winbanks CE, Chen JL, Qian H, Liu Y, Bernardo BC, Beyer C, et al. The bone morphogenetic protein axis is a positive regulator of skeletal muscle mass. J Cell Biol 2013;203(2): 345—57.
[35] Sartori R, Schirwis E, Blaauw B, Bortolanza S, Zhao J, Enzo E, et al. BMP signaling controls muscle mass. Nat Genet 2013; 45(11):1309—18.
[36] Clever JL, Sakai Y, Wang RA, Schneider DB. Inefficient skeletal muscle repair in inhibitor of differentiation knockout mice suggests a crucial role for BMP signaling during adult muscle regeneration. Am J Physiol Cell Physiol 2010;298(5): C1087—99.
[37] Friedrichs M, Wirsdoerfer F, Flohe SB, Schneider S, Wuelling M, Vortkamp A. BMP signaling balances proliferation and differentiation of muscle satellite cell descendants. BMC Cell Biol 2011;12:26.
[38] Ono Y, Calhabeu F, Morgan JE, Katagiri T, Amthor H, Zammit PS. BMP signalling permits population expansion by preventing premature myogenic differentiation in muscle satellite cells. Cell Death Differ 2011;18(2):222—34.
[39] Boon MR, van der Horst G, van der Pluijm G, Tamsma JT, Smit JW, Rensen PC. Bone morphogenetic protein 7: a broad-

spectrum growth factor with multiple target therapeutic potency. Cytokine Growth Factor Rev 2011;22(4):221—9.
[40] Singla DK, Singla R, Wang J. BMP-7 treatment increases M2 macrophage differentiation and reduces inflammation and plaque formation in apo E-/- mice. PLoS One 2016;11(1): e0147897.
[41] Zhong L, Wang X, Wang S, Yang L, Gao H, Yang C. The antifibrotic effect of bone morphogenic protein-7(BMP-7) on liver fibrosis. Int J Med Sci 2013;10(4):441—50.
[42] Midgley AC, Duggal L, Jenkins R, Hascall V, Steadman R, Phillips AO, et al. Hyaluronan regulates bone morphogenetic protein-7-dependent prevention and reversal of myofibroblast phenotype. J Biol Chem 2015;290(18):11218—34.
[43] Scherner O, Meurer SK, Tihaa L, Gressner AM, Weiskirchen R. Endoglin differentially modulates antagonistic transforming growth factor-beta1 and BMP-7 signaling. J Biol Chem 2007; 282(19):13934—43.
[44] Lee KB, Taghavi CE, Murray SS, Song KJ, Keorochana G, Wang JC. BMP induced inflammation: a comparison of rhBMP-7 and rhBMP-2. J Orthop Res 2012;30(12):1985—94.
[45] Kluk MW, Ji Y, Shin EH, Amrani O, Onodera J, Jackson WM, et al. Fibroregulation of mesenchymal progenitor cells by BMP-4 after traumatic muscle injury. J Orthop Trauma 2012; 26(12):693—8.